

# An efficient algorithm for kinematics estimation with application to dynamic gait stability using a contact-less skeleton tracking system

Michael Uelschen<sup>1</sup> <sup>a</sup>, Heinz-Josef Eikerling<sup>1</sup>, Sabrina Rbib and Helge Riepenhof<sup>2</sup>

<sup>1</sup>Faculty of Engineering and Computer Science, University of Applied Sciences Osnabrück, 49076 Osnabrück, Germany

<sup>2</sup>BG Klinikum Hamburg, Bergedorfer Str. 10, 21033 Hamburg, Germany

{m.uelschen, h.eikerling}@hs-osnabrueck.de, sabrina.rbib@outlook.de, helge.riepenhof@bgk-hamburg.de

**Keywords:** Gait Analysis, Kinematics Estimation, Marker-less Skeleton Tracking, Orthopaedic Technical Support

**Abstract:** This paper presents an optimized algorithm for estimating static and dynamic gait parameters. We use a marker- and contact-less motion capture system that identifies 20 joints of a person walking along a corridor. Based on the proposed gait cycle detection basic metrics as walking frequency, step/stride length, and support phases are estimated automatically. Applying a rigid body model, we are capable to calculate static and dynamic gait stability metrics. We conclude with initial results of a clinical study evaluating orthopaedic technical support.

## 1 INTRODUCTION


The precise monitoring of regaining walking ability after surgery treatment or the ability to compensate disabilities caused by injuries is of importance as this information can guide the rehabilitation process. In current clinical practice, dynamic stability is usually assessed using the Berg Balance Scale (Berg, Wood-Dauphinee, Williams, & Maki, 1992) and gait speed is usually assessed using the 10-meter walking test.

While these outcome measures have proven their applicability in daily clinical practice, they have some drawbacks for guiding the rehabilitation process or tailoring remedial provisions. First of all, the scores on the clinical scales do not show insight into the mechanisms that contribute to a potential improvement on the clinical scale. If for instance an increased dynamic balance is found on the Berg Balance Scale, it is not known whether this is the result of recovery of the affected leg or an increased use of the non-affected leg. The same applies for an increased gait speed as measured on the 10-meter walking test: it is unclear whether an increased gait speed is the result of an increased step length and/or an increased cadence (steps/min). Thus, a more detailed movement analysis based on measurable metrics would be of service.

Within research, dynamic stability has been increasingly quantified relating the position of the

body's center of mass (CoM) to the base of support (BoS). The base of support is composed of the two feet and the area between them. For elderly fallers it has been shown that they exhibit a different separation between the center of mass and base of support during walking, when compared to elderly non-fallers. This result suggests that the movement of the center of mass in relation to the base of support might enable the separation of fallers from non-fallers, which would be of high clinical relevance.

Tracking the movement of the center of mass in relation to the base of support, however, usually requires a fully instrumented gait analysis which is technically challenging, time-consuming and costly. Hence, the use of instrumented gait analysis in daily clinical practice is limited. Because of this, there is a demand for a system that is capable of measuring foot placement and center of mass plus is easy to use, fast to set up, and affordable. By quantifying foot placement, the system can also be used to detect whether an increased walking velocity is the result of an increased step length and/or an increased cadence. For characterizing a patient's gait according to the above measures, the DynMetrics (Eikerling, Uelschen, & Lutterbeck, 2016) system was extended to devise the above measures. The marker-less motion capturing system is capable of tracking foot placement and the body's center of mass by a network of optical sensor nodes.

<sup>a</sup> <https://orcid.org/0000-0002-0841-6954>

## 2 METHOD

### 2.1 Motion Capturing

The key algorithm was integrated into the contact-less and marker-less gait recognition system DynMetrics (Uelschen & Eikerling, 2015). The system permits to capture and analyse the gait of a subject along a walking corridor without any time-consuming preparation of the person caused e.g. by attaching markers. The system consists of a series of independent sensor nodes that record the movements of a person passing by. The constituent 3D data streams are fused into a single continuous skeleton stream which is based on a global coordinate system.

### 2.2 Algorithm Overview

The block diagram shown in Figure 1 outlines the proposed algorithm. The skeleton tracking system outputs a skeleton stream of a moving subject. The joints of each skeleton are used two-fold: (i) as input to the gait cycle detection, and (ii) as basis for the calculation of a rigid body model.

The control of postural stability or balance is an essential function in human movements. It is defined (Shumway-Cook & Woollacott, 2017) as a person's ability to keep the line of gravity passing through the center of mass within the base of support area beneath that person. In general movement tasks can be classified into static (sitting or standing) and dynamic (walking) stability.

In order to obtain these metrics, the center of mass is estimated beforehand. Finally, using the ankle positions the dynamic stability of gait is calculated.

The complete process is highly automated and does not require any interaction by the operator of the system (e.g. physical therapist). Therefore, we achieve a high degree of reproducibility.

### 2.3 Contribution

The contributions of this paper are: (i) a rigid body model that allows to derive CoM and that approximates the gold standard, (ii) the estimation of the gait frequency based on gait cycle detection using linear regression, (iii) the computation of stability metrics such as XCoM, and BoS based on the inverted pendulum model, and (iv) initial results on a clinical study evaluating orthopaedic footwear and orthotics.

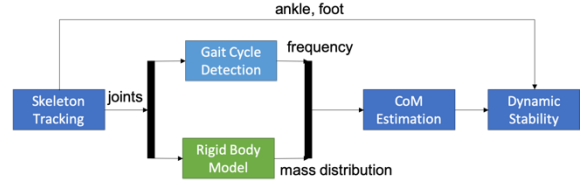


Figure 1: Pipeline algorithm.

## 3 GAIT CYCLE DETECTION

In this section we discuss the application of a peak-finding algorithm in order to identify the gait cycles. The estimated gait frequency (or alternatively cadence) is an input parameter for the subsequent stability assessment. The procedure uses the skeletal data gained by tracking a patient's movements. First, we explain the mathematical foundations.

### 3.1 Mathematical Preliminaries

The position in space  $r$  is given as, where  $t$  is the temporal parameter,

$$\vec{r}(t) = (x(t), y(t), z(t)) \quad (1)$$

We denote  $x$  as anterior-posterior (main moving direction),  $y$  as horizontal, and  $z$  as longitudinal axis. For the metrics of gait stability, often only the behavior in the horizontal plane is considered. That implies  $z(t) = 0$ .

The skeleton tracking system provides the position of the skeleton as a stream of frames at discrete points in time, which are given by  $t_i$  where  $i$  denotes the ordering of the frames in the sequence.

The skeleton tracking system estimates the position of twenty joints in each frame: head, shoulder center, spine, hip center, and in addition for both body sides: shoulder, elbow, wrist, finger, hip, knee, ankle, and toe. This raw data is the only input to the algorithm that estimates the kinematics and further gait metrics.

### 3.2 Gait Cycle

The recognition of individual steps is required to estimate the dynamic gait metrics. We follow the nomenclature given by (Perry & Burnfield, 2010).

The normal gait pattern is periodic, where a period corresponds to a single stride. According to Figure 2, adapted from (Götz-Neumann, 2015), each cycle can be divided into distinct phases.

The stance phase consists of five sub-phases followed by the swing phase. It is composed of three swing sub-phases before the gait cycle is completed. The identification of the gait phases provides important information for the clinical evaluation of a patient's gait pattern.

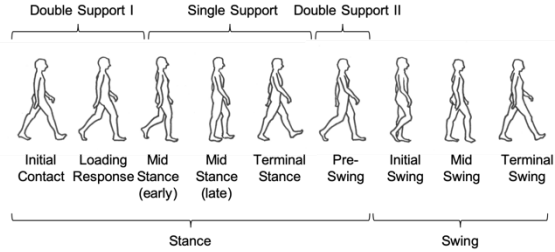


Figure 2: Gait cycle breakdown.

Below we describe an optimized procedure which automatically divides the movement into individual gait cycles.

Each phase of a cycle is started or ended by a defined event. Our algorithm identifies the following gait events: minimum, maximum and zero distances of the positions of the left and right ankle; maximum flexion of the ipsilateral and contralateral knee; and the vertical position of the lower limb (shank)

In order to find minimum or maximum values of a function  $v(t)$  we need to identify the peaks in usually noisy signal data. Under the assumption that  $v(t)$  has a periodic shape the automatic multiscale-based peak detection (AMPD) algorithm (Scholkmann, Boss, & Wolf, 2012) provides a stable approach. A major advantage of the algorithm is the absence of any problem-specific parameter, so that a specific tuning of the algorithm to the problem is not necessary. The stability and reliability are proved by several biomedical and non-biomedical applications.

In order to determine the individual gait phases, the movement of the person is first divided into

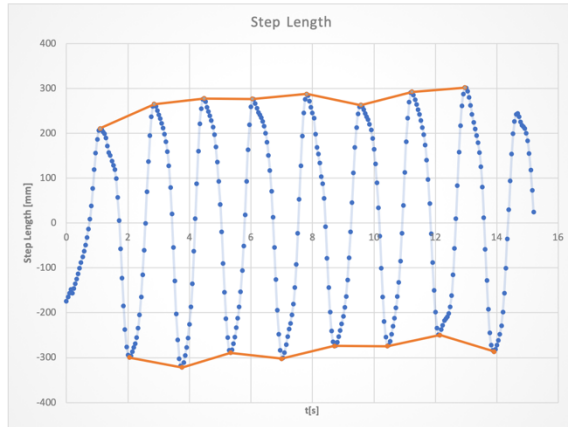


Figure 3: Peak detection using AMPD algorithm.

individual steps. The distance between the left and right ankle is used as the step length. A step is finished when the distance becomes maximum or minimum.

Figure 3 shows the AMPD algorithm detecting minimum and maximum distances of the left and right ankle. Due to the calculation method the algorithm may fail to find the initial or final peak.

Based on the detected gait cycles we can derive basic temporal-spatial parameters (TSP) as step/stride width and length, walking speed, and cadence given in steps per minute. The latter parameter can then be used to determine the gait frequency. These parameters are used for evaluation in the study described subsequently.

The transition from loading response to mid stance is triggered when the knee angle of the contralateral leg reaches its maximum value. The AMPD algorithm detects the peak values (see Figure 4) reliably even if the curve shows a more complex behaviour. The algorithm avoids to detect local extreme values.

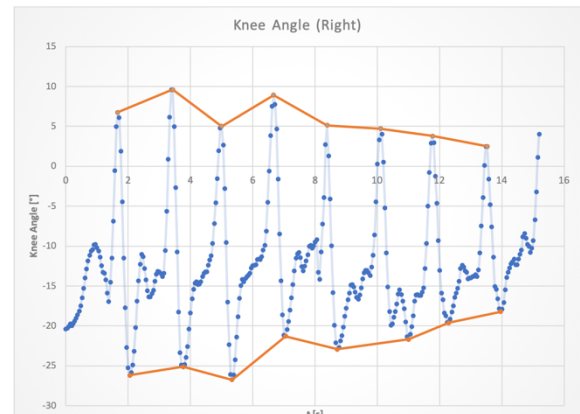


Figure 4: Detection of the flexion angle of the right knee.

## 4 GAIT STABILITY

The following section discusses how to derive the center of mass and gives a sinusoidal approximation based on the periodic walking pattern. This section ends with advanced metrics in order to evaluate the dynamic stability.

### 4.1 Rigid Body Model

In order to evaluate the stability of walking the center of mass is a relevant parameter. To determine this parameter, a body model is necessary, since the center of mass is very difficult to obtain directly. We use a segmented body model following the approach from (Hanavan, 1964). Based on the skeleton the body

segments are defined. Figure 5 shows on the left a 14-segment body model, e.g. the forearm segment is bound by the wrist and elbow joint. Each segment has an individual center of mass and a percentage weight.

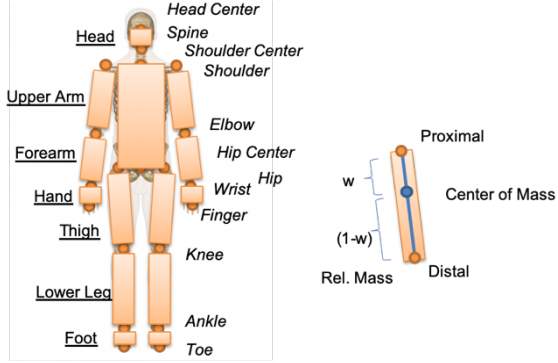


Figure 5: Segmented body model.

Finally, the overall center of mass is given by the weighted mean of all single segments (Winter, 2009). Table 1 summarizes the anthropometric data used for the estimation of segments' center of mass.

Table 1: Anthropometric data

Segment	Relative Mass	$w/(1-w)$
Head	7.0	
Trunk	43.0	0.60/0.40
Upper Arm	3.6	0.43/0.57
Forearm	2.2	0.43/0.57
Hand	0.7	0.30/0.70
Thigh	11.4	0.43/0.57
Lower Leg	5.3	0.43/0.57
Foot	1.8	0.43/0.57

The center of mass of each segment is defined by its relative location with respect to the proximal ( $w$ ) and distal ( $1 - w$ ) end point of the segment (see right part of Figure 5). For example, the forearm segment contributes 2.2% to the total mass. The segment is spanned by the elbow (proximal) and wrist (distal) joint of the skeleton. Its center of mass position is given by

$$\vec{r}_{\text{CoM, forearm}}(t) = 0.43 \cdot \vec{r}_{\text{elbow}}(t) + 0.57 \cdot \vec{r}_{\text{wrist}}(t) \quad (2)$$

## 4.2 Gold Standard Comparison

The sketched rigid body model is compared to a commercial marker-based motion capture system (Vicon) that represents the gold standard. The walking pattern of a person is recorded in parallel

using the DynMetrics and the Vicon system. The center of mass of both systems is compared and subsequently the deviation is analyzed. Vicon (VICON, 2017) uses a similar segmented body model as described, but the center of mass estimation is based on different anthropometric data. Due to the different local coordinate systems and the deviation of the internal clocks the comparison of both time series shows a shift in temporal and spatial direction (see Figure 6). Also, the field of view and the frames per second are varying.

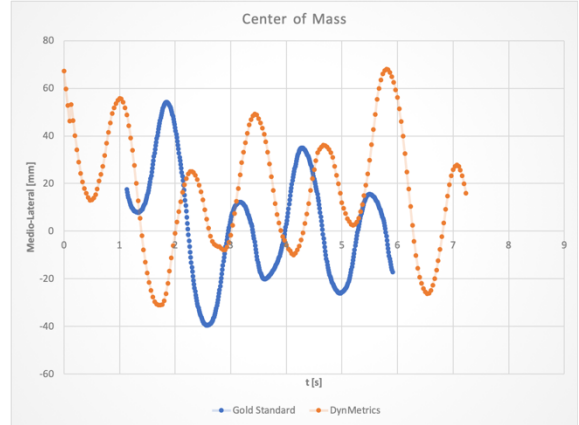


Figure 6: CoM estimation compared to gold standard.

In order to avoid such effects both data sets are aligned using an iterative closest-point algorithm. Figure 7 shows the aligned time series. The result indicates that DynMetrics estimates the body model similar to the gold standard.

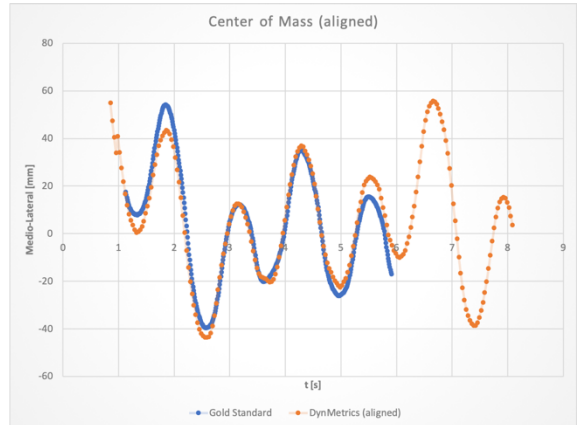


Figure 7: The aligned time series have similar shape.

## 4.3 CoM Sinusoidal Approximation

A relevant stability criterion is the medio-lateral displacement of CoM. Due to the periodic walking

pattern we approximate CoM as a simple harmonic motion within the horizontal plane, which is given as

$$y_{\text{CoM}}(t) = y_0 \cdot \sin(\omega t + \varphi_0) \quad (3)$$

The amplitude (displacement) is denoted by  $y_0$ , the angular frequency  $\omega = 2\pi f$ , and the phase angle  $\varphi_0$ . During several functional tests of our skeleton tracking system we observed that some subjects slightly turned to the left or to the right while walking. In order to get better approximation results we add this drift perpendicular to the motion in anterior-posterior direction. This results in the following model

$$y_{\text{CoM}}(t) = y_0 \cdot \sin(\omega t + \varphi_0) + a + m_0 t + m_1 t^2 \quad (4)$$

In order to estimate the unknown parameter, we use multiple linear regression method. Applying the angle addition theorem

$$\sin(x + y) = \sin x \cos y + \cos x \sin y \quad (5)$$

we can rewrite equation (3) as

$$\sin(\omega t + \varphi_0) = \sin(\omega t) \cos \varphi_0 + \cos(\omega t) \sin \varphi_0 \quad (6)$$

From this we derive the motion equation

$$y_{\text{CoM}}(t) = A_0 + A_1 \sin(\omega t) + A_2 \cos(\omega t) + A_3 t + A_4 t^2 \quad (7)$$

using

$$A_0 = a, A_1 = y_0 \cos \varphi_0, A_2 = y_0 \sin \varphi_0, A_3 = m_0, A_4 = m_1 \quad (8)$$

Based on  $n$  skeleton frames and applying the sketched body model  $(t_i, y_{\text{CoM},i})$  with  $i = 0, \dots, n - 1$  we get the following linear system of equations that can be solved using the least squares method. The vector representation is given by the following equation:

$$\vec{y}_{\text{CoM}} = B \cdot \vec{A} \quad (9)$$

with

$$\vec{y}_{\text{CoM}} = \begin{pmatrix} y_{\text{CoM},0} \\ y_{\text{CoM},1} \\ \vdots \\ y_{\text{CoM},n-1} \end{pmatrix} \quad (10)$$

$$B = \begin{pmatrix} 1 & \sin(\omega t_0) & \cos(\omega t_0) & t_0 & t_0^2 \\ 1 & \sin(\omega t_1) & \cos(\omega t_1) & t_1 & t_1^2 \\ \vdots & \vdots & \vdots & \vdots & \vdots \\ 1 & \sin(\omega t_{n-1}) & \cos(\omega t_{n-1}) & t_{n-1} & t_{n-1}^2 \end{pmatrix} \quad (11)$$

$$A = \begin{pmatrix} A_0 \\ A_1 \\ A_2 \\ A_3 \\ A_4 \end{pmatrix} \quad (12)$$

In order to find the solution equation (9) can be rewritten to

$$\vec{A} = (B^T B)^{-1} \cdot B^T \vec{y}_{\text{CoM}} \quad (13)$$

The motion in anterior-posterior direction of  $x_{\text{CoM}}(t)$  is approximately linear. Since the subject usually begins walking from double limb support with velocity  $v = 0$ , we apply the linear regression method to a polynomial of fourth degree. This gives better approximation results as a simple linear motion model. Figure 8 plots the behavior of center of mass in two variants. The first curve is based on the described body model. The second curve approximates the periodic oscillations in medio-lateral direction.

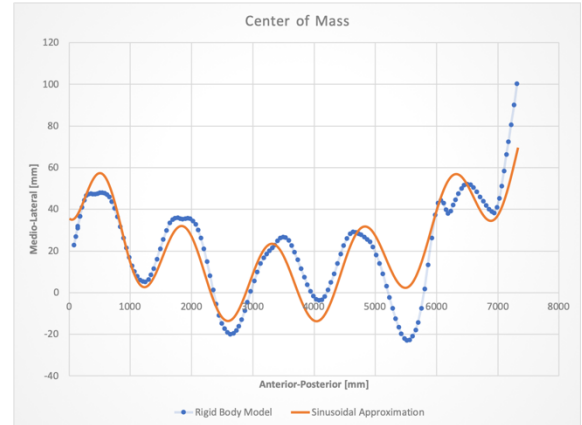


Figure 8: Center of mass exhibits sinusoidal behaviour.

#### 4.4 Dynamic Stability

CoM is an established stability metric in static situations. For the evaluation of the dynamic stability of gait we follow the approach by (Hof, Gazendam, & Sinke, 2005) that additionally considers the velocity of CoM  $v_{\text{CoM}}$  that leads to extrapolated CoM which is denoted as XCoM.



On the basis of the inverted pendulum model, XCoM adds an additional displacement to the center of mass position depending on the velocity of the person divided by  $\omega_0 = \sqrt{g/l}$ ,  $g$  being the acceleration of gravity and  $l$  leg length. The parameter  $\omega_0$  is the eigenfrequency of a non-inverted pendulum with length  $l$ .

The calculation of the dynamic gait stability therefore results in

$$x_{\text{XCoM}}(t) = x_{\text{CoM}}(t) + \frac{\dot{x}_{\text{CoM}}(t)}{\omega} \quad (14)$$

$$y_{\text{XCoM}}(t) = y_{\text{CoM}}(t) + \frac{\dot{y}_{\text{CoM}}(t)}{\omega} \quad (15)$$

using velocity  $v_{\text{CoM}} = (\dot{x}_{\text{CoM}}(t), \dot{y}_{\text{CoM}}(t))$ .

We approximate  $\omega$  using the gait frequency that results from the cycle detection. The literature shows different definitions of BoS, as for example in (Wu, Brown, & Gordon, 2017) the lateral position of the 5th metatarsal bone is used.

Our approach is similar to (Hak, van Dieën, van der Wurff, & Houdijk, 2014) using the position of the lateral malleolus. For the calculation of the base of support (BoS)  $\vec{s}(t)$  and afterwards the margin of stability (MoS)  $\vec{m}(t)$  we use the ankle position of the left  $\vec{r}_{\text{left}}(t)$  and right foot  $\vec{r}_{\text{right}}(t)$

$$\vec{s}(t) = \begin{cases} \vec{r}_{\text{left}}(t) & \text{left support} \\ \vec{r}_{\text{right}}(t) & \text{right support} \\ (\vec{r}_{\text{left}}(t) + \vec{r}_{\text{right}}(t))/2 & \text{double support} \end{cases} \quad (16)$$

Finally, the margin of support is the difference between the extrapolated CoM and BoS

$$\vec{m}(t) = \vec{r}_{\text{XCoM}}(t) - \vec{s}(t) \quad (17)$$

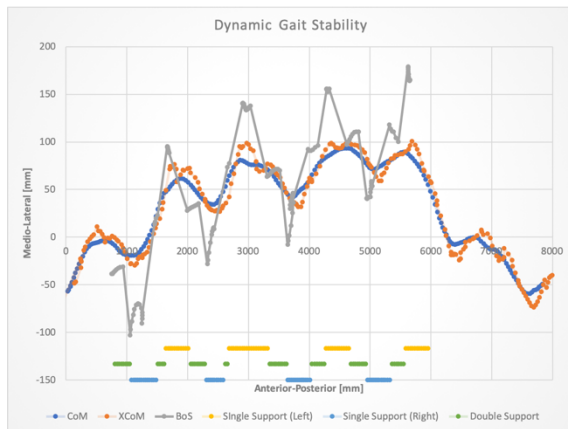


Figure 9: Dynamic gait stability.

The example in Figure 9 shows the dynamic stability metrics XCoM and BoS. In addition, the support phases are sketched below. The BoS curve oscillates in medio-lateral direction depending on the support phase.

## 5 ORTHOPAEDICS CASES



Figure 10: Walking corridor with four sensors on tripods.

### 5.1 Introduction

From an orthopaedics point of view, walking is a complex process. The gait cycle - as pointed out in section 3.2 - can be divided into different phases. This division permits to distinguish in detail physiological gait patterns from pathological forms and describe the observable deviations in a differentiated way. In addition, certain deficits in patients' feet or lower limbs can be at least partly compensated by supporting orthopedic aids. In particular, the provision of insoles or shoes tailored to the patient are common practical methods. The gait pattern of a healthy subject shows some specific parameters and all walking phases effect the main elements of walking, walking speed, cadence and stride length. Normally the gait patterns are periodic and fluent.

We have therefore extracted these elements from the DynMetrics data using, both with and without orthopedic additives (see (Götz-Neumann, 2015) for reference values): (i) walking speed, (ii) cadence and (iii) stride length. When people gain confidence while walking, they usually increase walking speed, cadence, and also stride length.

### 5.2 Method

Within a study we analysed the gait of 53 impaired subjects by means of the DynMetrics system. They

walked (see Figure 10) a distance of 8 m four times, twice with orthopaedic technical support such as custom-made insoles or adapted orthopaedic footwear and twice without any aids. In addition to the analysis of the gait, the subjects were asked assess the level of achiness while walking by means of the Visual Analog Scale (VAS) as shown in Figure 11.

The inclusion criterion of our investigation was that an orthopaedic dressing assumed to be medically indicated and that the orthopaedic compensation had already been assessed as fitting by the attending physician. Amputees were excluded from the study. In the study design, it was also determined that the test persons completed the four repetitions with and without orthopaedic preparation in random order.

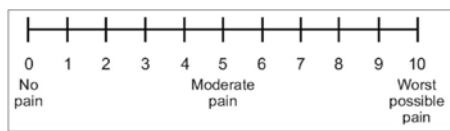


Figure 11: Visual Analog Scale (VAS)

### 5.3 Results

In subsequent discussion, the obtained results of two test persons will be used as examples to point out the change with respect to gait caused by using custom made orthopaedic footwear. Subject 1 is 44 years old, male. His dressing on the footwear includes a leg length compensation of 1 cm and a shaft stiffener.

Subject 2 is 56 years old, male and his dressing includes a heel elevation, shaft stiffening and rolling aid, as well as diabetic soft tissue bedding.

Table 2: speed, cadence, stride length and VAS number of subjects with and without orthopaedic additives

	Speed [m/min]	Cadence [1/min]	Stride Length [m]	VAS Number
<b>Subject 1</b>				
With additives	40.74	83.5	0.98	4
Without	34.16	84.2	0.81	5
Difference	<b>6.58</b>	<b>-0.7</b>	<b>0.17</b>	<b>-1</b>
<b>Subject 2</b>				
With additives	80.54	106.0	1.52	2
Without	72.80	112.4	1.30	3
Difference	<b>7.74</b>	<b>-6.4</b>	<b>0.22</b>	<b>-1</b>

Table 2 shows the arithmetic mean of the detailed measures. Both cases are similar with respect to the differences. There is increasing walking speed in both cases while using orthopaedic additives. Subject 1 covers the distance by 6.58 meters per minute and

subject 2 by 7.74 meters per minute. The stride length shows a similar pattern, both cases have an increased stride length. With increasing walking speed and stride length in both cases also the cadence decreases.

### 5.4 Discussion

As can be easily seen, painful walking influences the walking speed. With increasing pain, the walking speed decreases. The walking speed is mainly influenced by the stride length and cadence. The present study shows that the stride length increases with decreasing pain and the cadence decreases. This corresponds to the behavior of people with a physiological, painless gait pattern. It is therefore not to be assumed that the cadence is primarily increased by orthopedic adjustments, but rather by the stride length, which leads to a decrease in cadence at the same speed. There is clearly a reverse correlation between cadence and stride length. This means that as the cadence increases while the stride length decreases and vice versa in healthy and lower extremity disabled population.

Figure 12 shows the sway of subject 1. Due to larger stride length when using orthopaedic footwear, the oscillations are less dense. The medio-lateral displacement without using orthopaedic footwear is increased by 5 mm. From an orthopaedic point of view, trunk control indicated by the CoM oscillations essentially depends on the applicability of the deep trunk muscles (Van Criekinge, et al., 2017). The present investigations represented exclusively volunteers who had completed or are in the final phase of the rehabilitation process. At this point of therapy, a significant improvement in trunk stability should already have been achieved in any case, so that no significant changes are to be expected in the area of trunk control using orthopaedic aids.

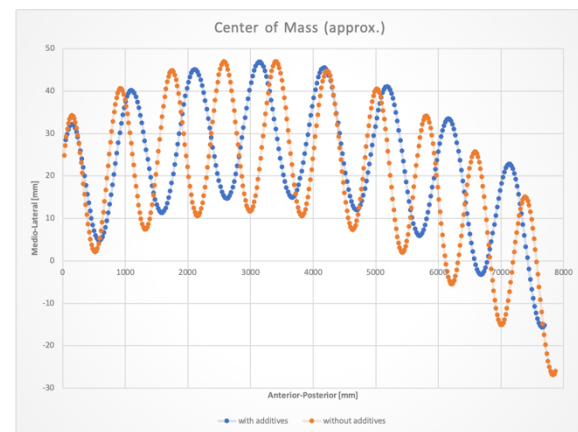


Figure 12: CoM depending on using orthopaedic additives.

## 6 CONCLUSIONS

In this paper we have presented a pipelined algorithm that derives temporal-spatial and dynamic gait parameters from skeletal data streams. Due to the marker- and contact-less approach and the resulting low effort the DynMetrics system which incorporates the devised algorithms is able to be used in daily clinical practice.

In order to give evidence for this we have used system to track gait improvements for patients in need of orthopaedic aids, i.e. according footwear and/or insoles. Specifically tailoring such aids to the individual patient is crucial to improve locomotion and avoid pain. It could be shown that by featuring the system the effect of using orthopedic additives can be captured by objective, quantitative metrics thus supporting the attending physician to direct the prescription of compensating measures. In our basic study we were able to nail down the differences in essential gait parameters for patients with and without those additives.

DynMetrics turned out to be suitable to capture the according data in reasonable time without major preparation effort. As expected, the additives can have a positive influence on the walking speed, stride length and cadence. Moreover, pain as measured by VAS can be lessened by the use of these additives. In addition to the use cases (orthopaedic and neurological rehabilitation), the presented algorithm can also be applied to other scenarios. Recently (Henderson, Gordon, & Vijayakumar, 2017) show that step width, medio-lateral displacement and BoS are invariant to walking conditions and may provide a robust metric in order to evaluate and compare wearable robots or exoskeletons.

## ACKNOWLEDGEMENTS

Partial support for the work was provided by Interreg-Project MIND No. 151131-R4-1.

## REFERENCES

- Berg, K. O., Wood-Dauphinee, S. L., Williams, J. I., & Maki, B. (1992). *Measuring balance in the elderly: validation of an instrument*. Canadian journal of public health, pp. 1073–1080. doi:ISSN 0003-9993
- Eikerling, H.-J., Uelschen, M., & Lutterbeck, L. (2016). *Scalable Distributed Sensor Network for Contact-less Gait Analysis - A Marker-less, Sensor-based System for Steering Rehabilitation Measures*. 9th International Joint Conference on Biomedical Engineering Systems and Technologies. Rome.
- Götz-Neumann, K. (2015). *Gehen verstehen* (4. Auflage). Stuttgart: Georg Thieme Verlag.
- Hak, L., van Dieën, J., van der Wurff, P., & Houdijk, H. (2014). *Stepping asymmetry among individuals with unilateral transtibial limb loss might be functional in terms of gait stability*. Physical Therapy, pp. 1480-1488.
- Hanavan, E. (1964). *A mathematical model of the human body*. Air force aerospace medical research lab Wright-Patterson AFB OH.
- Henderson, G., Gordon, D., & Vijayakumar, S. (2017). *Identifying invariant gait metrics for exoskeleton assistance*. 2017 IEEE International Conference on Robotics and Biomimetics (ROBIO). Macau.
- Hof, A., Gazendam, M., & Sinke, W. (2005). *The condition for dynamic stability*. Journal of Biomechanics, pp. 1-8.
- Perry, J., & Burnfield, J. (2010). *Gait Analysis* (2nd edition). Thorofare: SLACK Incorporated.
- Scholkmann, F., Boss, J., & Wolf, M. (2012). *An Efficient Algorithm for Automatic Peak Detection in Noisy Periodic and Quasi-Periodic Signals*. Algorithms, pp. 588-603.
- Shumway-Cook, A., & Woollacott, M. (2017). *Motor Control: Translating Research Into Clinical Practice* (5th ed). Philadelphia: Wolters Kluwer.
- Uelschen, M., & Eikerling, H.-J. (2015). *A Mobile Sensor System for Gait Analysis supporting the Assessment of Rehabilitation Measures*. Proceedings of the 6th ACM Conference on Bioinformatics, Computational Biology and Health Informatics (BCB '15) (pp. 96-105). New York: ACM.
- Van Crielinge, T., Saeys, W., Hallemans, A., Velghe, S., Viskens, P., Vereeck, L., . . . S., T. (2017, May). *Trunk biomechanics during hemiplegic gait after stroke: A systematic review*. Gait Posture, pp. 133-143. doi:10.1016/j.gaitpost.2017.03.004
- VICON. (2017). *Plug-In Gait Reference System*. Vicon Motion Systems.
- Winter, D. (2009). *Biomechanics and Motor Control of Human Movement* (4th edition). Hoboken: Wiley.
- Wu, M., Brown, G., & Gordon, K. (2017). *Control of locomotor stability in stabilizing and destabilizing environments*. Gait & Posture, pp. 191-196.